

Infrared thermal profiling and management of diseases affecting the biological cycle of *Antheraea assamensis* silkworm

Manasee Choudhury^{1,2,*} and Pranab Jyoti Das¹

¹Animal Genetics Laboratory, ICAR-National Research Centre on Pig, Rani, Guwahati 781 131, India

²Present address: Department of Zoology, Assam Don Bosco University, Tapesia, Guwahati 782 402, India

The present study has been designed to establish the thermal profile of complete life cycle of the *Antheraea assamensis* (muga) silkworms starting from the eggs to the moth. The current study also concurrently addresses the applicability of infrared thermography (IRT) to detect muga larvae infected with pebrine. Because of its non-contact advantage, IRT imaging can be successfully manoeuvred to reduce the risk of spreading infections and ultimately lead to increased silk production. The images and data obtained by the non-invasive IRT technology can be implemented, analysed and translated into deep learning algorithm-based machine learning called 'smart data', which can be fine-tuned to develop an artificial intelligence (AI) and decision support system (DSS) for the management and monitoring of silkworms in their entire life progression. Hence, this will boost their productivity, which will further revolutionize their yearly production and convey attractive revenues in the global silk picturesque.

Keywords: Decision support system, health status, infrared thermal imaging, muga silkworm, non-invasive.

SERICULTURE is the science of cultivating silkworms for the production of silk. However, one of the major hurdles faced by silk production industry is the onset of disease during silkworm rearing practice. Temperature challenges in the ecological biome distress most behavioural and physiological processes of insects, causing stress, injury and even death¹. Variations in the climatic factors significantly affect the genotypic expression of silkworms, causing changes in the phenotypic output of cocoon crops, such as cocoon weight, shell weight and cocoon shell ratio. Infrared thermal profiling can be proficiently propelled to measure the average surface heat of an organism and understand its body mechanism and functioning in response to behavioural and physiological changes at its thermo-neutral zone². Further, it can diagnose different diseases in a primordial state without disturbing the normal physiological conditions of the organism³. In the case of insects,

for measuring body temperature, using thermocouples has been the classical procedure for estimating the thermoregulatory ability of species⁴. However, as an invasive method, it has several limitations, such as a strong influence on the studied individuals, causing injuries or altering their behaviour⁵ and preventing the collection of reliable behavioural data associated with body temperature variations. Infrared thermography helps in taking incessant temperature measurements of several body parts noninvasively, without perturbing the animals' behaviour or social interactions^{6,7}.

With new inventions like smart machines and sensors cropping up in agriculture and other sectors of farming, surfacing technologies like the Internet of Things and cloud computing are introduced to leverage the transition from the traditional model of farming to artificial intelligence (AI)-based 'smart farming'⁸⁻¹¹. AI-based model, viz. NADRES v2 (National Animal Disease Referral Expert System version 2) has been developed to predict economically important livestock disease outbreaks in India and reduce its economic and social impact on the entire country¹². Infrared thermography has been reported as a new non-invasive machine learning technology in animal husbandry¹³. Similarly, decision support system (DSS) modules designed for use in livestock sector include Hot-Cross system for efficient livestock breeding¹⁴ and EpiMAN to check the control of contagious diseases¹⁵. It has also been developed in apiculture industries where the sound waves made by the bees can be tracked and hence can anticipate future changes to the swarm and the beehive¹⁶. The use of thermography for diagnosing contagious diseases and infections in farm and wild animals has been studied extensively for years¹⁷. However, scientific evidence on the successful application of infrared thermography (IRT) in thermal profiling of healthy and diseased insects, especially silkworms is minimal. Therefore, the present study reports the use of digital infrared thermography to establish the thermal profiling of the biological stages of healthy muga silkworm crop starting from the eggs to the moth. The study also reports the surface body temperature of diseased larvae responsible for poor performance and insufficient silk production.

*For correspondence. (e-mail: manasc25@gmail.com)

Material and methods

Collection of samples

Eggs of muga silkworm were procured from local silk rearers in and around Guwahati, India. Muga is semi-domestic in nature, and its rearing is executed both in the outdoor phase and indoor phase. The rearing of silkworms was carried out in Khanapara Silk Farm, Guwahati (in natural farm conditions) while cocooning of the larvae functioned in ICAR-National Research Centre on Pig, Guwahati, India (indoor conditions).

Infrared thermal camera

The infrared thermal images of different biological stages of muga silkworms were recorded using a forward-looking infrared (FLIR) camera, model no. T62101 with the software FLIR Research IR Max 4. The emissivity and focal distance of the camera for each stage were kept fixed throughout the investigation, viz. at 0.95 and 30 cm respectively. IRT images were captured from a total of 180 silkworms during different times (morning and afternoon) of the day.

Infrared thermal imaging

The thermal pictograms of the muga larvae were taken in a natural farm environment along with their standalone host plants. The mature, ripen 5th instar larvae were later collected and placed amidst dry plant leaves to proceed to their next biological stage, viz. the building of cocoons in indoor conditions. Some of the mature cocoons were dissected to record the thermal temperature of the pupa, while rest of the cocoons were left undisturbed to meet the adult moth stage. The adult moths (both male and female), after copulation, further laid eggs and died, thus completing the life cycle. In addition, IRT images were also captured from silkworm larvae naturally infected with pebrine disease during the experiment.

The ambient temperature range considered at the time of investigation was 23–28°C and relative humidity recorded was 65–80%. No parts of the insect were in contact with any hot or cold sources during the entire study. The white or red images in a thermogram represent the warmest, and the blue or black area represents the coolest part of the object, and variations in colour pattern signify thermal gradients, which denote changes in surface skin temperature due to underlying factors¹⁸.

Results and discussion

Muga silkworm is a holometabolous insect that undergoes a complete metamorphosis from egg to adult moth stage

through two intermediate stages of larva and pupa (Figure 1). The optimum temperature reported for normal growth of silkworms is about 20–28°C, and the temperature found to be effective for maximum productivity ranges from 23°C to 28°C (ref. 19). Temperature beyond the optimal range instantaneously affects the health of the silk species, causing the worms to become too weak and susceptible to various diseases¹⁹. During the present study, the IRT temperature of 1st, 2nd and 3rd instar larva was perceived to be $30.26 \pm 0.33^\circ\text{C}$, $30.74 \pm 0.25^\circ\text{C}$ and $31.67 \pm 0.53^\circ\text{C}$ respectively (Table 1). The average thermal readings of 4th and 5th instar larva were recorded to be $28.49 \pm 0.22^\circ\text{C}$ and $27.98 \pm 0.79^\circ\text{C}$ respectively (Table 1). The increased surface body heat of the younger instars synchronizes with the fact that they are voracious eaters, grow very vigorously and lead to a high growth rate compared to 4th and 5th instar phase²⁰. The early instars contain the resistance to sustain the elevated surrounding temperature, which assists in improving the survival rate and cocoon characteristics. The digested food in the first three instars is consumed as the energy required for their growth and movement during feeding¹⁹. The growth rate of silkworm larva is maximal in 3rd instar, moderate in 4th and minimal

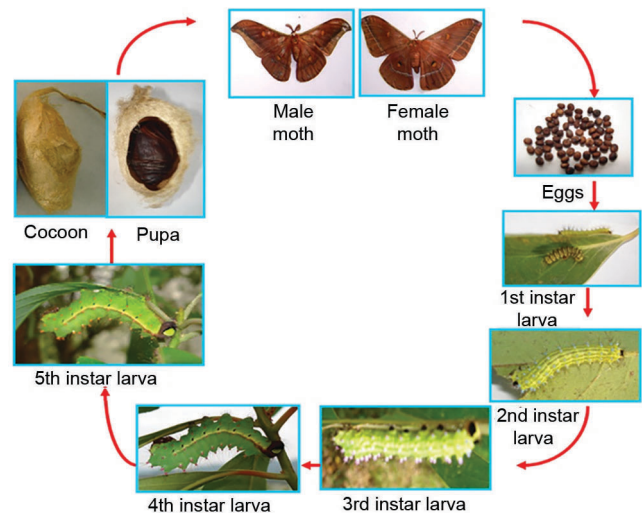


Figure 1. Complete life cycle of muga silkworm (*Antheraea assamensis*).

Table 1. Infrared thermal values of muga larvae during different instar stages

Muga larval stage	IRT value recorded
1st instar larvae	$30.26 \pm 0.33^\circ\text{C}$
2nd instar larvae	$30.74 \pm 0.25^\circ\text{C}$
3rd instar larvae	$31.67 \pm 0.53^\circ\text{C}$
3rd instar moulting larvae	$27.51 \pm 0.95^\circ\text{C}$
4th instar larvae	$28.49 \pm 0.22^\circ\text{C}$
5th instar larvae	$27.98 \pm 0.79^\circ\text{C}$
5th instar larvae during cocoon formation	$29.76 \pm 0.16^\circ\text{C}$

Mean \pm SD = 180.

in 5th stage, though the spurts in larval body weights in absolute terms reflect the opposite trend²¹. Figures 2 and 3 *a* show the infrared thermal images of 3rd, 4th and 5th instar muga larva respectively. The larvae use absorbed nutrients to provide energy for growth and development, during which they synthesize and secrete a large amount

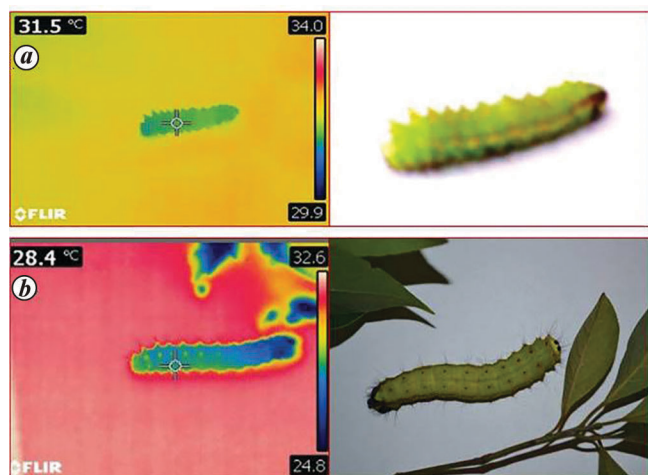


Figure 2. Muga silkworm at (a) 3rd instar larval stage and (b) 4th instar larval stage.

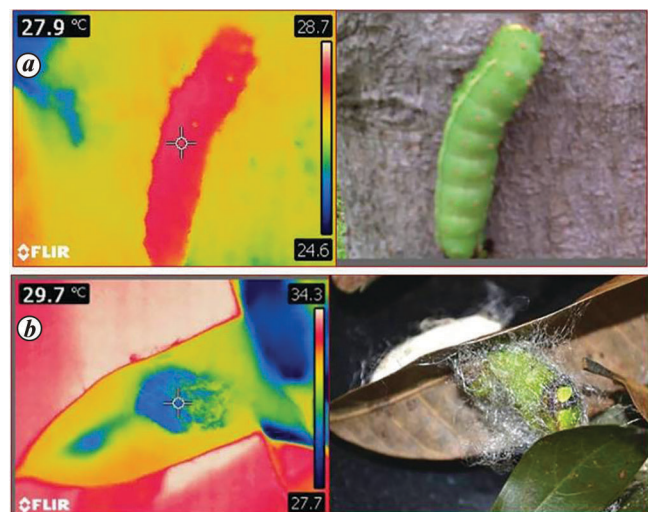


Figure 3. Muga silkworm at (a) 5th instar larval stage and (b) 5th instar larva at the time of cocoon formation.

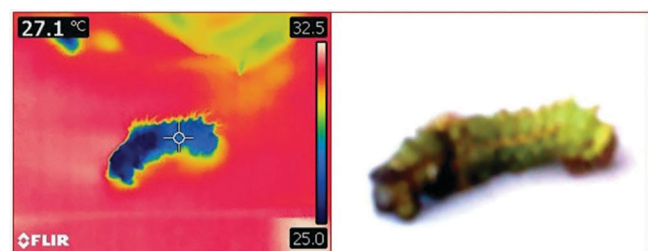


Figure 4. Moulting larva of muga silkworm at 3rd instar stage.

of silk proteins²². In the last stage of 5th instar, the larva loses appetite, stops feeding, and becomes yellowish and mature. The matured larva later finds for itself a suitable place for cocoon fabrication. At the time of cocoon architecture, the infrared surface body temperature of the 5th instar larva was observed to be $29.76 \pm 0.16^\circ\text{C}$ (Figure 3 *b*). In addition, the current observation also captured the surface body heat of a 3rd instar moulting larva at $27.51 \pm 0.95^\circ\text{C}$ (Figure 4), which is lower than the normal motile larva. At this phase, the creature stops feeding, and other movement activity ceases, characterized by low activity levels in all the tissues, which parallels with the present lower IRT reading of the moulting larva compared to the normal healthy stage.

The energy reserves mounted up in the larval fat body during their feeding phases are later deployed for the growth, metamorphosis and nourishment of the new adult. Silkworm pupa and moth depend on these reserves for their sustenance and reproduction. Thermal investigations carried out on live muga cocoons (with pupa inside) interpreted its surface heat at $26.54 \pm 0.36^\circ\text{C}$ (Figure 5 *a* and Table 2). Surface heat radiated from the pupal body is recorded at $27.58 \pm 0.41^\circ\text{C}$ (Figure 5 *b* and Table 2). The average body temperature of the pupa is found to be less than the active larval period. It is apparent as the worms become lethargic and enter a sleep-like quiescent state during which there is a cessation of feeding and movement,

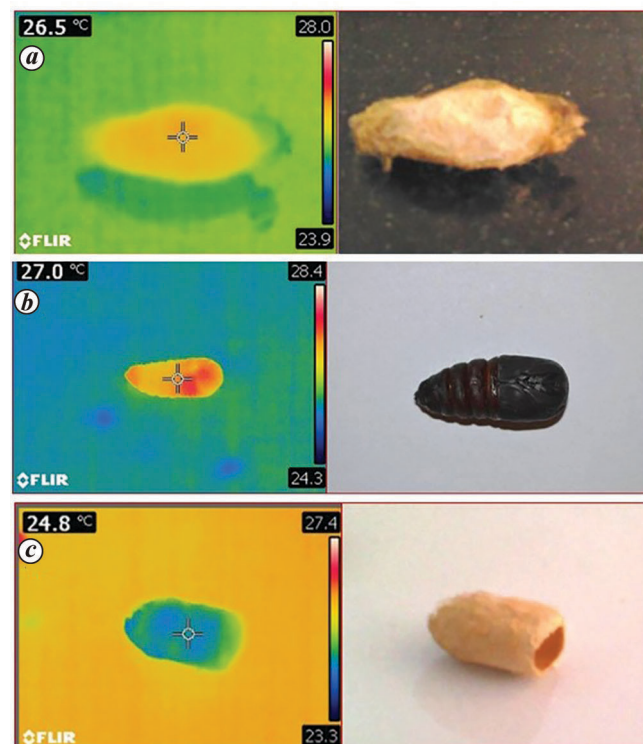


Figure 5. *a*, Live cocoon of muga silkworm (with pupa inside). *b*, Live pupa of muga silkworm. *c*, Cut cocoon of muga silkworm (without pupa).

and larval food reserves are drawn upon for energy. In the course of the larval pupal transition, the growth falls remarkably due to complete utilization of silk gland proteins for cocoon-spinning at the end of 5th instar and subsequent disintegration of both gut and silk glands during the early pupal phase.

Thermal pictograms of adult muga moth just after emergence from cocoons have recorded temperature at 25.73 ± 0.36 for male and $26.49 \pm 0.79^\circ\text{C}$ for female (Table 3). Infrared images of male and female muga moths are shown in Figure 6 *a* and *b* respectively. A further decline in weight was observed during the pupal-adult transition period. The decline is more pronounced in males than in females, attributed to the fact that males need more energy for courtship (wing beating) and copulatory behaviours, compared to females²³. After emergence, the adult is incapable of flight because of its feeble wings and heavy body, and its only role is copulation, followed by laying eggs in case of females. It does not feed during its short

Table 2. Infrared thermal temperatures of muga cocoons and pupa

Muga cocoons with/or without pupa	IRT value recorded
Muga cocoons (with pupa inside)	$26.54 \pm 0.36^\circ\text{C}$
Muga pupa	$27.58 \pm 0.41^\circ\text{C}$
Muga cocoon shells (without pupa)	$25.05 \pm 0.55^\circ\text{C}$

Mean \pm SD = 180.

Table 3. Infrared thermal temperatures of muga silkworm and muga eggs

Different stages of muga silkworm	IRT value recorded
Muga silk moth (male)	$25.73 \pm 0.36^\circ\text{C}$
Muga silk moth (female)	$26.49 \pm 0.79^\circ\text{C}$
Muga eggs	$24.2 \pm 0.21^\circ\text{C}$

Mean \pm SD = 180.

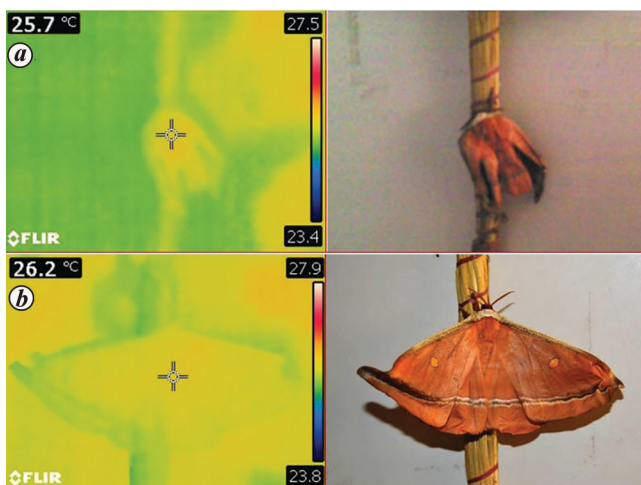


Figure 6. *a*, Male muga moth after emergence from cocoon. *b*, Female muga moth at the time of laying eggs.

adult life, and the only medium of energy is drawn from its larval reserves. It reveals that IRT value of the laid eggs was found to be $24.2 \pm 0.21^\circ\text{C}$ (Figure 7 and Table 3), while Figure 5 *c* displays that temperature radiated from the empty cocoon shell immediately after the emergence of adult moth was measured to be $25.05 \pm 0.55^\circ\text{C}$ (Table 2). The present observation establishes the normal thermographic profile of the complete life cycle of muga silkworm. IRT can be exquisitely used to monitor the health status of muga throughout its cycle. Furthermore, IRT can sharply detect the 5th instar ripe larva (before the stage of cocoon formation) and aid the farmers in their timely transfer to indoor conditions for cocoon fabrication to save the larvae from the attack of predators and pests in the outdoor state.

The current study also concurrently tries to manifest thermal imaging to study the surface body temperature of muga larvae infected with pebrine. Pebrine is one of the deadliest diseases caused by the protozoan *Nosema bombycis*, resulting in severe damage to the silkworm crop and wreaking economic havoc on the silk industry. The infection takes place in a bimodal form: firstly, in the course of trans-ovarian transmission causing vertical infection from the mother moth through infected eggs²⁴, making it the primary course of infection, and secondly, by the ingestion of contaminated host plant leaves leading to secondary horizontal contamination. In most cases, the frequent source of contagion is bought by the ingestion of food (muga plant leaves) contaminated with microsporidians by silkworms. The symptoms of protozoan attacked larva include losses in appetite, retarded growth, irregular moulting and appearance of small pepper-like black-brown spots on their skin. The IRT thermograms of pebrine infected larva of the 3rd and 5th instar have evidenced elevated body heat at $30.62 \pm 0.13^\circ\text{C}$ and $30.32 \pm 0.05^\circ\text{C}$ (Table 4) respectively, compared to the normal healthy larva (Figure 8). The rise in temperature of the body is a consequence of prevailing infections inside the insect. A sequence of biochemical and physiological alterations take place in the host body²⁵. Such changes due to the pervading pathogen in the larva indicate high metabolic stress ensuing in increased body temperature. The source of contagion is primarily through the faeces of diseased silkworms and dead larvae, pathogens prevailing in rearing environments, grainage houses and appliances, and the contaminated

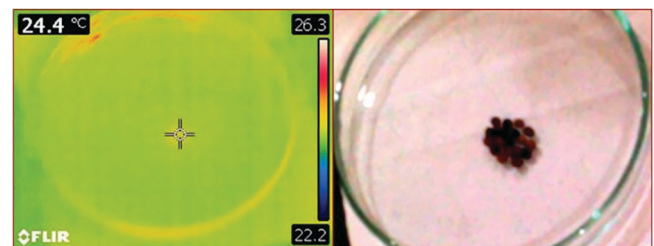


Figure 7. Eggs laid by the mother muga moth.

host plants and infected eggshell surfaces. These pathogens are highly stable and persistent for a longer span in the rearing environment. Bracing the spread of such infectious diseases is hard to meet due to the nature of transmission and resistance of the microbes against antimicrobial drugs²⁶. Several physical and chemical disinfectants have been adopted in sericulture farms to ensure eradication of the pathogen. Kagawa²⁷ and Reddy *et al.*²⁸ reported the use of chemical disinfectants and antibiotics for managing the disease in silkworms. However, the chemical-based disinfectants and drug formulations used for deterrence and control of this disease are not economical or eco-friendly and have many limitations to being effective in open and outdoor rearing practices. It has been regarded as an expedient method to measure surface temperature endlessly without contracting or stressing the species and with minimal risk of injuries²⁹. The thermal profiling of the entire biological cycle of muga silkworms established in this study by the IRT technology can be further oriented to develop a deep learning algorithm based machine learning DSS for monitoring and management of the health of the silkworms at each specific stage. With the help of DSS, the healthy diseased free larvae can be screened and selected for silk production, while the comparatively less healthy, diseased and infected one, causing extensive loss to the silk trade, can be promptly discarded at the very onset. These data can be used as a baseline to translate conventional farming into smart farming and develop an AI system to detect different stages of the larva and their disease condition in a rapid time, which can finally increase the accuracy of detecting silkworm diseases and their physiological changes related to the economic return of silk farming. In addition to pebrine, some of the other common diseases responsible for the yearly economic downfall of the sericulture industry are flacherie, green muscardian, gracherie, etc. Such technology can prove to be a promising antidote to alleviate non-invasively the

suffering caused by such pathogens by allowing timely diagnosis and encouraging healthy silk crop production, ultimately leading to silk production par excellence. Thermal imaging has been executed for pest detection in their grain storage³⁰. It is reported to be an easier and enhanced alternative to prevent an insect infestation than to treat an established infestation. IRT imaging has spotted invasion of pests like rusty grain beetle, cowpea seed beetle, white pine cone beetle, Australian fire-beetle, citrus long-horned beetle, woodworm and red palm weevil in their respective host plants. This is perceived as the respiration of insects, resulting in higher heat production than the grain³¹⁻³³. In animals, this technique has proved to be particularly advantageous in the early detection of foot diseases³⁴ and mastitis³⁵ in dairy cows and oestrous detection in pigs³⁶, allowing timely prediction and diagnosis, which improved animal welfare, as well as reducing the economic loss for the farmer.

Conclusion

Thermal profiling of living species is indispensable to assess their growth and development, along with their behavioural and physiological reflexes at their thermo-tolerance level. Use of thermography to detect health status in silkworms is a very new concept. The present investigation is the first such report on the use of digital infrared thermography to establish thermal profile of the complete life cycle of muga silkworms. Further, this study also conducted basic thermographic differences between healthy muga larvae and larvae infected with deadly pebrine contagion. Though thermography in the current study is limited to revealing specific pathological details of the infected larvae, it can be a reliable tool in identifying the diseased larvae potentially infected with pebrine by defining the area of inflammation and/or injury or increased metabolism or decrease in body heat. The observed thermal temperature of the silkworms evidenced in the study can be further calibrated to establish a smart data-based machine learning DSS for the monitoring and screening muga silkworms at different stages of their biological cycle, which will augment their biological productivity annually. In the current landscape, IRT can function as a possible panacea by being the first line of defence to contain the spread of diseases that cause bulky economic loss to silk textile production. Therefore, IRT can be maneuvered as an automatic surveillance state-of-the-art technology for smart farming, disease detection and upsurge productivity in silkworms on the global silk platform.

Conflict of interest: The authors declare that there is no conflict of interest.

Table 4. Infrared thermal values of pebrine infected muga larvae at different instar stage

Diseased larvae	IRT value recorded
Pebrine infected larvae in 3rd instar stage	30.62 ± 0.13°C
Pebrine infected larvae in 5th instar stage	30.32 ± 0.05°C

Mean ± SD = 50.

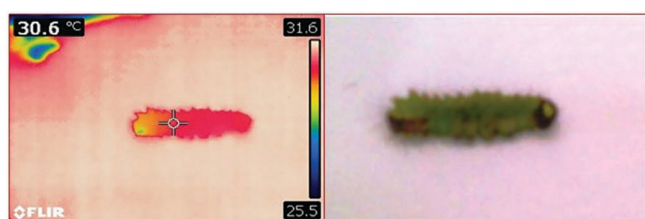


Figure 8. Pebrine infected muga larva at 5th instar stage.

1. Cossins, A., In *Temperature Biology of Animals*, Springer Science and Business Media, Berlin, 2012, pp. 1-22.

2. Soerensen, D. D. and Pedersen, L. J., Infrared skin temperature measurements for monitoring health in pigs: a review. *Acta Vet. Scand.*, 2015, **57**, 1–11.
3. Knižková, I., Kunc, P., Gürdil, G. A. K., Pinar, Y. and Selvi, K. C., Applications of infrared thermography in animal production. *J. Fac. Agric.*, 2007, **22**, 329–336.
4. Heinrich, B., Social thermoregulation. In *The Hot-Blooded Insects*, Springer, Berlin, Heidelberg, 1993, pp. 447–509.
5. Watt, W. B., Accuracy, anecdotes, and artifacts in the study of insect thermal ecology. *Oikos*, 1997, **80**, 399–400.
6. Stabentheiner, A. and Schmaranzer, S., Thermographic determination of body temperatures in honey bees and hornets: calibration and applications. *Thermology*, 1987, **2**, 563–572.
7. Chown, S. L. and Nicolson, S., *Insect Physiological Ecology: Mechanisms and Patterns*, Oxford University Press, London, 2004.
8. Sundmaeker, H., Verdouw, C., Wolfert, S. and Pérez Freire, L., Internet of food and farm 2020. In *Digitising the Industry – Internet of Things Connecting Physical, Digital and Virtual Worlds* (eds Vermesan, O. and Friess, P.), River Publishers, Gistrup/Delft, 2016, pp. 129–151.
9. Wolfert, S., Ge, L., Verdouw, C. and Bogaardt, M. J., Big data in smart farming – a review. *Agric. Syst.*, 2017, **153**, 69–80.
10. Vander Waal, K., Morrison, R. B., Neuhauser, C., Vilalta, C. and Perez, A. M., Translating big data into smart data for veterinary epidemiology. *Front. Vet. Sci.*, 2017, **4**, 110.
11. Fu, Q., Shen, W., Wei, X., Zhang, Y., Xin, H., Su, Z. and Zhao, C., Prediction of the diet energy digestion using kernel extreme learning machine: a case study with Holstein dry cows. *Comput. Electron. Agric.*, 2020, **169**, 105231.
12. Suresh, K. P., Hemadri, D., Kruli, R., Dheeraj, R. and Roy, P., Application of artificial intelligence for livestock disease prediction. *Indian Farming*, 2019, **69**, 60–62.
13. Choudhury, M. *et al.*, Infrared imaging a new non-invasive machine learning technology for animal husbandry. *Imaging Sci. J.*, 2020, **68**(4), 240–249.
14. Newman, S., Lynch, T. and Plummer, A. A., Success and failure of decision support systems: learning as we go. *J. Anim. Sci.*, 2000, **77** (E-Suppl.), 1–12.
15. Jalvingh, A. W., Nielen, M., Dijkhuizen, A. A. and Morris, R. S., EpiMAN: decision support system for contagious animal disease control. *IFAC Proc. Vol.*, 1995, **28**, 97–102.
16. Marr, B., How artificial intelligence, IoT and big data can save the bees, 2020; https://specialsimages.forbesimg.com/imageserve/5e9fc586dea8300007de8a08/960_x0.jpg?fit=scale (accessed on 22 April 2020).
17. Cilulko, J., Janiszewski, P., Bogdaszewski, M. and Szczygielska, E., Infrared thermal imaging in studies of wild animals. *Eur. J. Wildl. Res.*, 2013, **59**(1), 17–23.
18. Eddy, A. L., Van Hoogmoed, L. M. and Snyder, J. R., The role of thermography in the management of equine lameness. *Vet. J.*, 2001, **162**, 172–181.
19. Ueda, S., Theory of the growth of silkworm larvae and its application. *Jpn. Agric. Res. Q.*, 1982, **15**, 180–184.
20. Muthunagai, M., Comparative study on the feeding activity of *Bombyx mori* with host plants *Morus nigra* (mulberry) and alternative plant *Ricinus communis* (Castor Plant). *IOSR J. Agric. Vet. Sci.*, 2016, **9**, 29–33.
21. Tanaka, K., Uda, Y., Ono, Y., Nakagawa, T., Suwa, M., Yamaoka, R. and Touhara, K., Highly selective tuning of a silkworm olfactory receptor to a key mulberry leaf volatile. *Curr. Biol.*, 2009, **19**, 881–890.
22. Zhang, W., Chang, X. Q., Hoffmann, A., Zhang, S. and Ma, C. S., Impact of hot events at different developmental stages of a moth: the closer to adult stage, the less reproductive output. *Sci. Rep.*, 2015, **5**, 10436.
23. Burger, M., Jacob, A. and Kropf, C., Copulatory behavior and web of *Indicoblemma lannaianum* from Thailand (Arachnida, Araneae, Tetrablemmidae). *J. Arachnol.*, 2006, **34**, 176–185.
24. Ishihara, R. and Fujiwara, T., The spread of pebrine within a colony of the silkworm, *Bombyx mori* (Linnaeus). *J. Invertebr. Pathol.*, 1965, **7**, 126–131.
25. Bergold, G. H., Insect viruses. In *Adv. Virus. Res. 1* (eds Smith and Luaffer), Academic Press, New York, 1963, pp. 91–139.
26. Nenaah, E. G. and Ahmed, M. E., Antimicrobial activity of extracts and latex of *Calotropis procera* (Ait.) and synergistic effect with reference antimicrobials. *Res. J. Med. Plant.*, 2011, **5**, 706–716.
27. Kagawa, T., The efficacy of formalin as disinfectant of *Nosema bombycis* spores. *J. Sericult. Sci. Jpn.*, 1980, **49**, 218–222.
28. Reddy, R. M., Sinha, M. K. and Prasad, B. C., Application of parental selection for productivity improvement in tropical tasar silkworm *Antheraea mylitta* Drury – a review. *J. Entomol.*, 2010, **7**, 129–140.
29. Islam, M. M., Ahmed, S. T., Mun, H. S., Bostami, A. R., Kim, Y. J. and Yang, C. J., Use of thermal imaging for the early detection of signs of disease in pigs challenged orally with *Salmonella typhimurium* and *Escherichia coli*. *Afr. J. Microbiol. Res.*, 2015, **9**, 1667–1674.
30. Al-doski, J., Mansor, S. B., Shafri, H. Z. B. M. and Zulhaidi, H., Thermal imaging for pests detecting a review. *Int. J. Agric. For. Fish.*, 2016, **2**, 10–30.
31. Cofie-Agblor, R., Muir, W. E., Zhang, Q. and Sinha, R. N., Heat of respiration of *Cryptolestes ferrugineus* (Stephens) adults and larvae in stored wheat. *Can. Agric. Eng.*, 1996, **38**, 37–44.
32. Damecveski, K. A., Annis, P. C. and Waterford, C. J., Effect of grain on apparent respiration of adult stored-product Coleoptera in an air-tight system: implications for fumigant testing. *J. Stored Prod. Res.*, 1998, **34**, 331–339.
33. Emekci, M., Navarro, S., Donahaye, E., Rindner, M. and Azrieli, A., Respiration of *Rhizopertha dominica* (F.) at reduced oxygen concentrations. *J. Stored Prod. Res.*, 2004, **40**, 27–38.
34. Redaelli, V., Tarantino, S., Ricci, C., Luzi, F., Zeconi, A. and Verga, M., A non-invasive method to measure the lameness in dairy cows. *Ital. J. Anim. Sci.*, 2009, **8**, 671.
35. Berry, R. J., Kennedy, A. D., Scott, S. L., Kyle, B. L. and Schaefer, A. L., Daily variation in the udder surface temperature of dairy cows measured by infrared thermography: potential for mastitis detection. *Can. J. Anim. Sci.*, 2003, **83**, 687–693.
36. Saara, C. S., Clark, S. G., Knox, R. V. and Tamassia, M. A., Vulvar skin temperature changes significantly during estrous in swine as determined by digital infrared thermography. *J. Swine Health Prod.*, 2011, **19**, 151–155.

ACKNOWLEDGEMENTS. We acknowledge the financial support from the Department of Biotechnology-Research Associateship Program in Biotechnology and Life Sciences, GOI. We also thank the Director, ICAR-NRC on Pig, Guwahati, India, for granting permission to carry out the research.

Received 11 March 2024; revised accepted 29 April 2024

doi: 10.18520/cs/v127/i2/232-237